

Can we resolve 3D density heterogeneity in the lower mantle?

Barbara Romanowicz,

Berkeley Seismological Laboratory, Berkeley, California.

Abstract. We reexamine the possibility of resolving 3D density structure in the mantle, by performing test inversions using a dataset of well constrained degree 2 splitting coefficients. We show that degree 2 in V_s and V_p can be resolved, and confirm that $dlnV_s/dlnV_p > 2.5$ at depths > 2000 km, indicating a chemical component to large scale heterogeneity. Models with ρ positively correlated with V_s in the deepest mantle fit the data at least as well as those in which density and velocities are anti-correlated. However, some rough bounds on $dln\rho/dlnV_s$ can be inferred. Models obtained from geodynamic considerations are acceptable, in contrast to models with large negative (< -0.3) or positive (> 0.6) $dln\rho/dlnV_s$ throughout the lower mantle. The most robust feature is a marked increase in $dln\rho/dlnV_s$ at the top of the lower mantle reaching a maximum around 1500 km.

1. Introduction

A recent study by *Ishii and Tromp* [1999] has revived a long-lasting controversy regarding whether or not lateral variations in density in the mantle can be constrained using normal mode data. In principle, low angular degree normal modes are sensitive to 3D structure in all three elastic parameters: V_s , V_p , and density (ρ). However, the sensitivity to ρ is significantly smaller than that to V_s or V_p , making it difficult to resolve even the 1D mantle density profile (e.g. *Kennett* [1998]), and casting doubts as to the feasibility of resolving ρ in 3D.

Using a collection of normal mode splitting data to test inversions for 3D elastic structure up to degree 8, *Resovsky and Ritzwoller* [1999] showed that the resulting density distribution depends strongly on a priori constraints on the model parametrization and regularization. Recently, *Kuo and Romanowicz* [2000] inverted normal mode spectral waveforms to illustrate how, depending on the parametrization and the starting models in V_s and V_p , significantly different final density models can be obtained. In the latter study, lateral structure up to spherical harmonics degree 6 was considered.

A prominent feature of the *Ishii and Tromp* [1999] model is that high density regions correspond to low seismic velocities, in the central Pacific and under Africa, in the bottom 200-500 km of the mantle. If robust, this structure bears important implications for the dynamics and mineral physics of the mantle [e.g. *Karato and Karki* 2000]. This feature has a strong degree 2 component. Since higher order normal mode splitting coefficients are still subject to large

measurement uncertainties, whereas different authors agree on the values of most degree 2 coefficients, we reanalyze the degree 2 data to try and further clarify the issue of resolution of 3D density structure in the mantle. This analysis also allows us to confirm the behavior, at the longest wavelengths, of the ratio $R_{s/p} = dlnV_s/dlnV_p$, which appears to increase with depth in the lower mantle [e.g. *Robertson and Woodhouse*, 1995; *Su and Dziewonski*, 1997].

2. Dataset and Model Parametrization

Degree 2 splitting coefficients were measured recently by *Resovsky and Ritzwoller* [1998], *He and Tromp* [1996], and *Durek and Romanowicz* [1999] for spheroidal modes, *Tromp and Zankerka* [1995] and *Resovsky and Ritzwoller* [1998] for toroidal modes. We only consider mantle modes with no sensitivity in the inner core. We exclude modes for which measurements differ significantly between authors. In particular, only 13 toroidal modes are kept, for which at least two compatible measurements exist, or for which the unique measurement agrees with the predictions of the SH tomographic model SAW12D [*Li and Romanowicz*, 1996]. Several layered parametrizations are considered. Data are corrected for crustal structure using an isostatically compensated Moho model based on Etopo5 topography and bathymetry. As shown previously, [*Romanowicz and Bréger*, 2000], the details of the crustal corrections have no incidence on the lower mantle structure retrieved. Since the resolution of this low angular order splitting dataset is poor in the upper mantle, we focus the discussion on the lower mantle results.

In our inversions, we consider overall norm damping parameters that can be adjusted separately for V_s , V_p and ρ as well as for topography of the 670-km discontinuity (d670) and the core-mantle boundary (CMB). No regularization scheme is applied to better assess where instabilities arise in the models. The damping parameters are adjusted so that (1) on average, the amplitudes of the depth profiles of individual degree 2 coefficients in V_s match those of recent S tomographic models; (2) $R_{s/p} = dlnV_s/dlnV_p$ matches the range of 1.5 to 2 predicted by mineral physics and obtained in previous studies in the top 1500km of the mantle; (3) when inverting independently for density, $R_{\rho/s} = dln\rho/dlnV_s$ is on average between 0.2 and 0.3 in the mid-mantle, compatible with predictions from geodynamics and mineral physics studies [e.g. *Forte and Woodward*, 1997; *Karato and Karki*, 2000]; (4) the C20 component of the CMB topography has a value comparable with that inferred from astronomical observations [*Gwinn et al.*, 1986]. Assigning the same damping parameter to V_s and V_p obtains (2) without further adjustments, which is an indication that V_p can be resolved independently of V_s . However, to obtain (3), ρ needs to be damped at least twice as much, and the resulting profile of $R_{\rho/s}$ is much less regular.

Copyright 2001 by the American Geophysical Union.

Paper number 1999GL012278.
0094-8276/01/1999GL012278\$05.00

3. Results

In Figures 1 and 2, we compare the depth profiles of $R_{s/p}$, $R_{\rho/s}$, and of the corresponding correlation coefficients, obtained for different parametrizations of the mantle, when V_s , V_p and ρ are inverted for independently, with (Figure 1) or without (Figure 2) allowing for topography on the CMB. Table 1 lists the fits to the data for these and other models. All models have a stable $R_{s/p}$ down to about 1800 km, increasing to values > 3 below that depth. This ratio decreases again near the CMB. V_s and V_p are well correlated throughout the lower mantle. However, the correlation between ρ and V_s is less stable with depth, as is $R_{\rho/s}$. Models with or without topography on the d670 give similar fits to the data, and exhibit similar profiles in the lowermost mantle. When topography on the CMB is allowed, there is a positive correlation of ρ and V_s in the last 1000 km of the mantle (Figure 1). When no CMB topography is allowed, $R_{\rho/s}$ becomes negative in the bottom 500km of the mantle, and the fit to the data is poorer (Table 1). The negative correlation between ρ and V_s seen in the mid lower mantle in some models depends on the parametrization and is therefore not a robust feature.

In order to investigate further whether the ρ structure obtained is well constrained, we have conducted a set of experiments, in which we prescribe $R_{\rho/s}$ throughout the mantle, and invert the data independently for V_s and V_p . We start with a depth profile of $R_{\rho/s}$ compatible with geodynamic [Forte and Woodward, 1997] or mineral physics [Karato, 1993] considerations. Figure 3 shows the same depth profiles as in Figures 1 and 2, where we compare an inversion

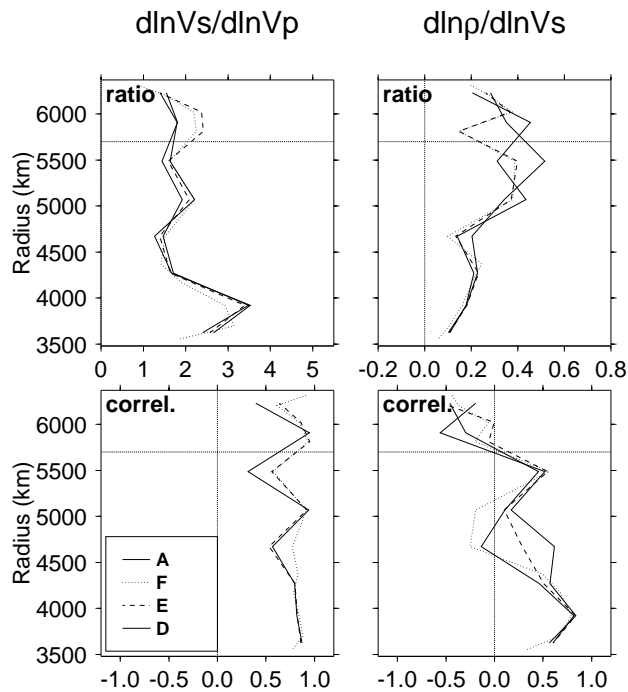


Figure 1. Depth profiles for $R_{p/s}$ and $R_{\rho/s}$ and correlation coefficients between V_s and V_p (left) and ρ and V_s (right) for four models obtained by independently inverting for V_s , V_p and ρ , with different parametrizations in the mantle (see Table 1), allowing for topography on the CMB. In model A, topography on the d670 is allowed, but not in other models shown.

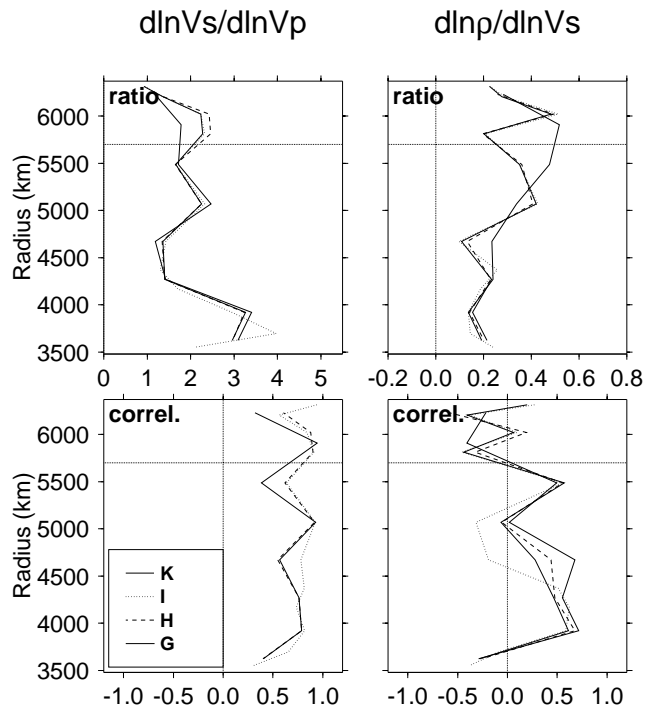


Figure 2. Same as Figure 1, for models in which topography on the CMB is not allowed.

obtained without constraints on ρ (D), with inversions in which $R_{\rho/s}$ is given respectively as, that of Forte and Woodward, [1997] (D1), the same profile modified in the deepest

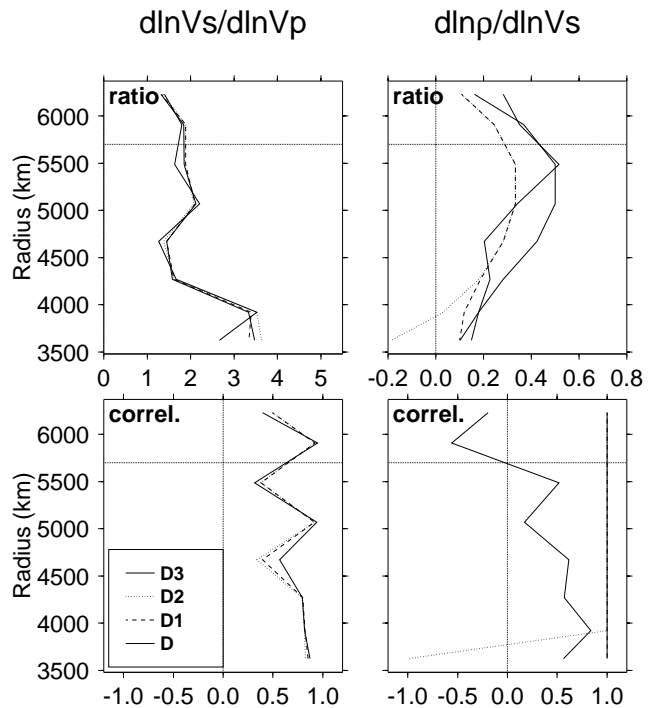


Figure 3. Depth profiles for $R_{p/s}$ and $R_{\rho/s}$ and correlation coefficients between V_s and V_p (left) and ρ and V_s (right) for model D and three models (D1,D2,D3) obtained by imposing the ρ/V_s profile (see Table 1).

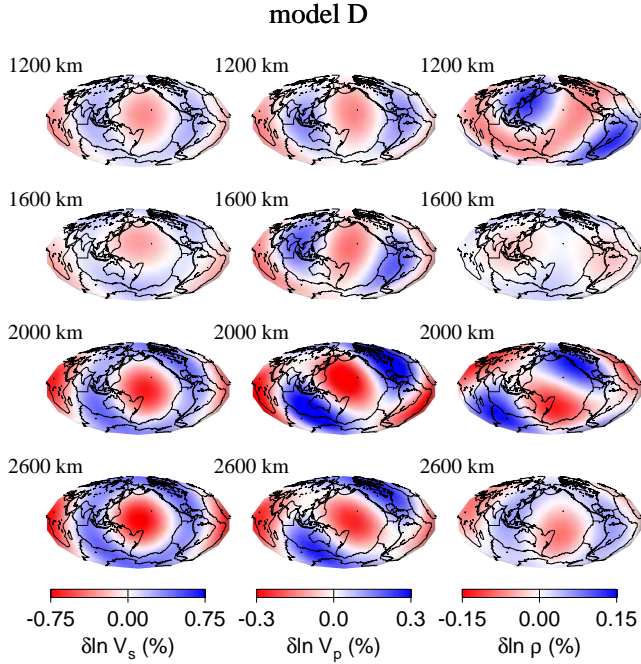


Figure 4. Maps of degree 2 in V_s , V_p and ρ at representative depths in the lower mantle, for model D.

500 km to obtain a negative $R_{\rho/s}$ (D2), and the same profile with $R_{\rho/s}$ multiplied by a factor of 1.5 throughout the mantle (D3). Figure 3 shows that $R_{s/p}$ is stable, as is the corresponding correlation. In fact, further inspection shows that both V_s and V_p models are quite stable in these inversions, except in the lowermost mantle, where imposing constraints on the density profile results in even larger $R_{s/p}$ values, indicating some trade-offs between velocity and density. The fits to the data (Table 1) show that, as expected, independently inverting for velocities and density yields slightly better fits to the data than when imposing constraints on density. This is however not significant, given the errors in the data and

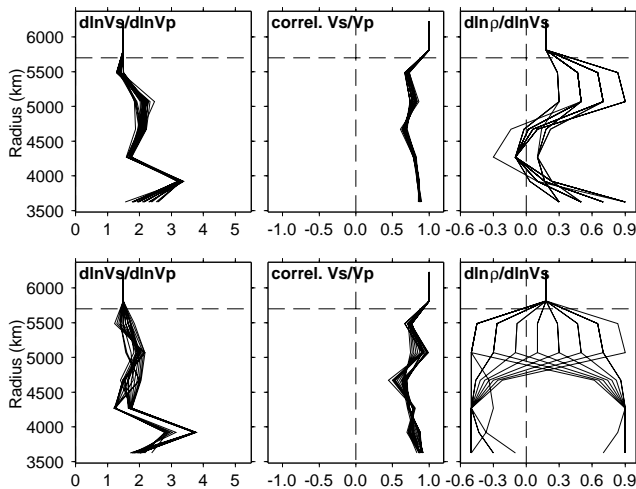


Figure 5. From left to right: $R_{p/s}$, correlations between V_s and V_p , and $R_{\rho/s}$, as a function of depth, for the 20 best (top) and 20 worst (bottom) models discussed in text. In all cases, the layer parametrization is the same as for model C shown in Table 1.

Table 1. Characteristics of models shown in Figures 1, 2 and 3: number of layers in upper and lower mantle, allowance for CMB topography, whether or not the ρ/V_s profile is constrained and residual variance (%)

Model	up. mant.	lo. mant.	670km	CMB	constr. on ρ	res. var.
A	2	6	yes	yes	no	5.95
B	3	6	yes	yes	no	5.98
C	4	8	yes	yes	no	6.10
D	2	6	no	yes	no	6.06
D1	2	6	no	yes	yes ^a	6.45
D2	2	6	no	yes	yes ^b	6.50
D3	2	6	no	yes	yes ^c	6.45
E	3	6	no	yes	no	6.01
F	4	8	no	yes	no	6.14
G	2	6	no	no	no	6.60
H	3	6	no	no	no	6.55
I	4	8	no	no	no	6.79
J	2	6	no	yes	yes ^d	6.55
K	4	6	no	no	no	6.60

^a $R_{\rho/s}$ profile of Forte and Woodward [1997].

^bSame $R_{\rho/s}$ profile as in ^a modified in lowermost mantle.

^cSame $R_{\rho/s}$ profile as in ^a multiplied by 1.5.

^dDensity model of Ishii and Tromp[1999]

larger number of degrees of freedom in the latter case. On the other hand, the three density profiles tested yield indistinguishable fits to the data, as does a model in which the 3D degree 2 density structure is constrained to be that of *Ishii and Tromp* [1999] (Table 1, model J). In the latter case, the V_s and V_p models exhibit similar features to other models.

Figure 4 shows maps of V_s , V_p and ρ at representative lower mantle depths for model D (independent inversion for V_s , V_p and ρ). The velocity maps are in good agreement with the degree 2 part of global tomographic S velocity [e.g. *Li and Romanowicz*, 1996] or P velocity [e.g. *Bolton*, 1996] models.

The tests shown here indicate that, while degree 2 in V_s and V_p is well resolved throughout the lower mantle, this is not the case for ρ . In particular, currently available normal mode data are unable to resolve the degree 2 $R_{\rho/s}$ in the lower mantle to within a factor of 2, nor a change of sign in the correlation between ρ and V_s in the lowermost mantle. However, on average, the $R_{\rho/s}$ profiles obtained without a priori constraints on density (except for overall damping) are in good agreement with geodynamically plausible models of density.

To further investigate whether we can impose some bounds on the density profile in the lower mantle, without constraints from damping, we performed a parameter search experiment. We investigated values of $R_{\rho/s}$ ranging from -0.5 to 0.9 in the depth ranges 670-1500, 1500-2500, 2500-2900km respectively. Since our dataset is not very sensitive to upper mantle structure, we fixed $R_{\rho/s}=0.18$ and $R_{s/p}=1.5$ in the upper mantle. We inverted for V_s and V_p independently in the lower mantle, allowing for CMB and d670 topography. We verified in another set of experiments (not shown), that models with $R_{\rho/s} < 0.3$ are preferred in the upper mantle.

Figure 5 shows the depth profiles of the 20 best and 20 worst models obtained. The best models fit is within 0.5% of the best fitting model, whereas the worst models have 11-15% larger residual variance than the best fitting model. Figure 5 shows the following, regarding the degree 2 in $R_{\rho/s}$: (1) there is a marked increase between the upper mantle and the top of the lower mantle (where preferred values are between 0.3 and 0.9). In the mid-lower mantle, the ratio generally decreases to small positive or negative values. Only models with large negative (or positive) $R_{\rho/s}$ in the bottom 500km can be ruled out, as models with $|R_{\rho/s}| < 0.3$ yield fits to the data that are only a few percent poorer than the best fitting models. The preferred profiles are compatible with those based on geodynamics or mineral physics (e.g. Figure 3). The poorest models present a more oscillatory $R_{s/p}$ profile.

4. Discussion and Conclusions

Our results show that degree 2 V_s and V_p structure is independently well resolved. The ratio $R_{s/p}$ increases significantly below 2000km depth, confirming earlier results. Additional tests, with a parameter search on $R_{s/p}$ and fixed $R_{\rho/s}$, confirm this trend, although the variance reduction achieved in such experiments is not as good as in the experiments shown in Table 1, indicating that the assumption of perfect correlation of V_p , V_s and ρ is too strong.

In a study based on body wave travel times, Bolton [1997] observed that a particular region in the Pacific Ocean was primarily responsible for the anomalously large $R_{s/p}$ in the lowermost mantle. However, the global coverage was rather uneven. The fact that we observe this in degree 2 indicates that there is a global, large scale component of heterogeneity in the lowermost mantle that cannot be explained by thermal effects alone.

Structure in ρ , even at the longest wavelengths is not well resolved. When ρ is inverted for independently of V_s and V_p , the sign of $R_{\rho/s}$ in the bottom 500km of the mantle trades off with topography on the CMB. Density models based on geodynamics and mineral physics inferences are compatible with the data, whereas models with amplitudes of density heterogeneity exceeding the latter by a factor of 2 or more can be ruled out. The mode splitting data alone cannot resolve the existence of high density "blobs" in the central Pacific and under Africa, as proposed by Ishii and Tromp [1999]: models with positive correlation between ρ and V_s in the lowermost mantle yield slightly, but not significantly, better fits to the data, but small negative $R_{\rho/s}$ in the lowermost mantle cannot be ruled out. Whereas Ishii and Tromp [1999] also used free air gravity data to constrain the amplitude of lateral variations in density, such constraints are very weak. In particular, they depend on the dynamic topography assumed for major discontinuities and/or details of the viscosity profile in the mantle. Our attempts to discriminate between models using fits to the gravity data have not been successful.

The most robust feature of the degree 2 in ρ is the increase in $R_{\rho/s}$ at the top of the lower mantle, reaching a

maximum in the depth range 1000-1500km. Below that depth $|R_{\rho/s}| < 0.3$, but its sign is not well constrained.

Acknowledgments. The author thanks A. Forte for providing his profile of $R_{\rho/s}$, as well as for fruitful discussions, and S. Karato for sharing his paper in advance of publication. This study was partially supported by NSF Grant EAR9902777. BSL contribution #0008.

References

- Bolton, H., Long period travel times and the structure of the Mantle, PhD Thesis, Univ. of Calif. San Diego, 1996.
- Durek, J., and B. Romanowicz, Inner core anisotropy inferred by direct inversion of normal mode spectra, In press *Geophys. J. Int.*, 139, 599-622, 1999.
- Dziewonski, A. M., and D.L. Anderson, Preliminary reference Earth model, *Phys. Earth Planet. Inter.*, 25, 297-356, 1981.
- Forte, A.M. and R. L. Woodward, Seismoc-geodynamic constraints on three-dimensional structure, vertical flow and heat transfer in the mantle, *J. Geophys. Res.*, 102, 17981-17994, 1997.
- Gwinn, C. R., T. A. Herring, and I.I. Shapiro, Geodesy by radio interferometry: Studies of the forced nutations of the Earth, 2 Interpretation, *J. Geophys. Res.*, 91, 4755-4765, 1986.
- He, X. and J. Tromp, Normal-mode constraints on the structure of the Earth, *J. Geophys. Res.*, 101, 20,053-20,082, 1996.
- Ishii, M., and J. Tromp, Normal-mode and free-air gravity constraints on lateral variations in velocity and density of Earth's mantle, *Science*, 285, 1231-1236, 1999.
- Kennett, B. L. N., On the density distribution within the earth, *Geophys. J. Int.*, 132, 374-382, 1998.
- Li, X. D., and B. Romanowicz, Global mantle shear velocity model developed using nonlinear asymptotic coupling theory, *J. Geophys. Res.*, 101, 22,245-22,272, 1996.
- Karato, S., Importance of anelasticity in the interpretation of seismic tomography, *Geophys. Res. Lett.*, 20, 1623-1626, 1993.
- Karato, S. and B. Karki, Origin of variation of seismic velocities in the deep mantle, submitted to *J. Geophys. Res.*, 2000.
- Kuo, C. and B. Romanowicz, On the resolution of density anomalies in the Earth's mantle using spectral fitting of normal mode data, *Geophys. J. Int.*, submitted, 2000.
- Resovsky, J. S., and M. H. Ritzwoller, New and refined constraints on 3-D Earth structure from normal modes below 3 mHz, *J. Geophys. Res.*, 103, 783-810, 1998.
- Resovsky, J. S., and M. H. Ritzwoller, Regularization uncertainty in density models estimated from normal mode data, *Geophys. Res. Lett.*, 26, 2319-2322, 1999.
- Robertson, G. S. and J. H. Woodhouse, Evidence for proportionality of P and S heterogeneity in the lower mantle, *Geophys. J. Int.*, 123, 85-116, 1995.
- Romanowicz, B., and L. Bréger, Anomalous splitting of free oscillations: a reevaluation of possible interpretations, *J. Geophys. Res.*, in press, 2000.
- Su, W. and A.M. Dziewonski, Simultaneous inversion for 3-D variations in shear and bulk velocity in the mantle, *Phys. Earth Planet. Inter.*, 100, 135-156, 1997.
- Tromp, J., and E. Zankerka, Toroidal splitting observations from the great 1994 Bolivia and Kuril Islands earthquakes, *Geophys. Res. Lett.*, 22, 2297-2300, 1995.

B. Romanowicz, Berkeley Seismological Lab, Berkeley, CA, 94720, USA. (e-mail: barbara@seismo.berkeley.edu)

(Received August 30, 2000; revised December 13, 2000; accepted December 18, 2000.)